

Tulinsky, A., Vandlin, R. L., Morimoto, C. N., Mani, N. V., & Wright, L. H. (1973) *Biochemistry* 12, 4185-4192.
 Ugurbil, K., Maki, A. H., & Bersohn R. (1977) *Biochemistry* 16, 901-907.
 von Schütz, J. U., Zuclich, J., & Maki, A. H. (1974) *J. Am. Chem. Soc.* 96, 714-718.

Wetlaufer, D. B. (1973) *Proc. Natl. Acad. Sci. U.S.A.* 70, 697-701.
 Wetlaufer, D. B., & Ristow, S. (1973) *Annu. Rev. Biochem.* 42, 135-158.
 Zuclich, J., Schweitzer, D., & Maki, A. H. (1973) *Photochem. Photobiol.* 18, 161-168.

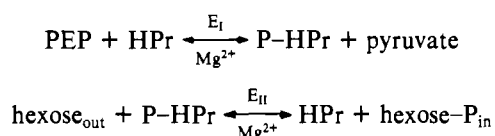
Escherichia coli Phosphoenolpyruvate-Dependent Phosphotransferase System. Evidence That the Dimer Is the Active Form of Enzyme I[†]

O. Misset, M. Brouwer, and G. T. Robillard*

ABSTRACT: In vitro kinetic measurements have been performed by using purified HPr, E_I, and a membrane fraction of E_{II} from the *Escherichia coli* phosphoenolpyruvate-dependent sugar transport system. These measurements reveal very large lag times in the formation of methyl α -glucoside phosphate which are a function of the E_I and the E_{II} concentrations. The lag times decrease with increasing concentrations of E_I but they

increase with increasing concentrations of E_{II}. When E_I, together with Mg²⁺ and phosphoenolpyruvate, is preincubated at 37 °C before starting the kinetic measurements, the lag time can be decreased or eliminated. We have shown that the process responsible for the lag time is the activation of E_I by dimerization which is influenced by Mg²⁺ and phosphoenolpyruvate.

The *Escherichia coli* phosphoenolpyruvate-dependent phosphotransferase system is responsible for the concomitant phosphorylation and transport of PTS¹ sugars across the cytoplasmic membrane (Roseman, 1969; Kundig & Roseman, 1971; Postma & Roseman, 1976). The energy source, PEP, is coupled to the phosphorylation and transport processes by a minimum of two enzymatic reactions:



Procedures have been developed for the complete purification of a number of the proteins in this system (Anderson et al., 1971; Dooijewaard et al., 1979a; Robillard et al., 1979). As a result of these developments, it is now possible to begin studies on the molecular details of the energy coupling and transport mechanism, their regulation, and the kinetics which describe the individual processes. Initial studies on the mechanism of energy coupling have recently been reported (Dooijewaard et al., 1979b). In this present study the kinetics of the phosphorylation of methyl α -glucopyranoside have been monitored under conditions where the rate-limiting component has been HPr and E_I or E_{II}. Lag times in α -MeGlc-P formation on the order of several minutes to 1 h were encountered. These could be made a function of the E_I and E_{II} concentrations. These lag times are orders of magnitude longer than the millisecond to second lag times commonly encountered during the establishment of a steady state in an enzymatic reaction. Since pre-steady-state kinetics can help clarify a reaction sequence, subsequent measurements on the origin of these lag times were performed. The results obtained indicate

that the observed lag times are due to a slow self-association of E_I to an active dimeric form.

Materials and Methods

Bacteria. *E. coli* K 235 and *Salmonella typhimurium* SB 2950 were grown and harvested as stated previously (Dooijewaard et al., 1979a).

HPr was purified from *E. coli* K 235 according to the procedure of Dooijewaard et al. (1979a).

E_I was purified from *E. coli* K 235 by the method of Robillard et al. (1979). The ethylene glycol was removed by gel filtration over Sephadex G-75 after which the E_I was stored at -20 °C in the lyophilized form.²

E_{II}. The source of E_{II} was the cytoplasmic membrane fraction of *S. typhimurium* SB 2950. Frozen cells were resuspended in 25 mM Tris-HCl buffer, pH 7.5, 1 mM DTT, and 1 mM NaN₃ (1 g wet weight cells/5 mL of buffer) and passed through a French pressure cell at 10 000-15 000 psi. The cell debris was removed by centrifugation for 30 min at 48000g. The supernatant was subjected to high-speed centrifugation (200000g for 2 h) to collect the membrane pellet. This pellet was washed once after resuspending in the same buffer to the original volume. The final pellet was resuspended in 20% of the original crude cell extract volume by using the same buffer and frozen at -20 °C until use.

Assay Procedure. The phosphorylation reaction was carried out at 37 °C in a final volume of 225 μ L containing the following components: 5 μ mol of potassium phosphate, pH 7.5; 2.5 μ mol of KF; 0.25 μ mol of DTT; 2 μ mol of PEP (cyclohexylammonium salt); 2 μ mol of methyl α -glucopyranoside containing an amount of methyl α -D-[U-¹⁴C]glucopyranoside sufficient to produce 200 000 cpm/ μ mol of α -MeGlc; 0.5 μ mol of MgCl₂; 0.2 nmol of HPr; the specified amounts of E_I and E_{II}. After being incubated at 37 °C, the phosphorylated sugar

[†] From the Department of Physical Chemistry, University of Groningen, Nijenborgh 16, 9747 AG Groningen, The Netherlands. Received September 6, 1979. This research has been supported by the Netherlands Foundation for Chemical Research (S.O.N.) with financial aid from the Netherlands Organization for the Advancement of Pure Research (Z.W.O.).

¹ Abbreviations used: PEP, phosphoenolpyruvate; α -MeGlc, methyl α -glucopyranoside; PTS, phosphoenolpyruvate-dependent phosphotransferase system; DTT, dithiothreitol.

² E_I purified by this procedure may be associated with ribonucleic acid (unpublished results).

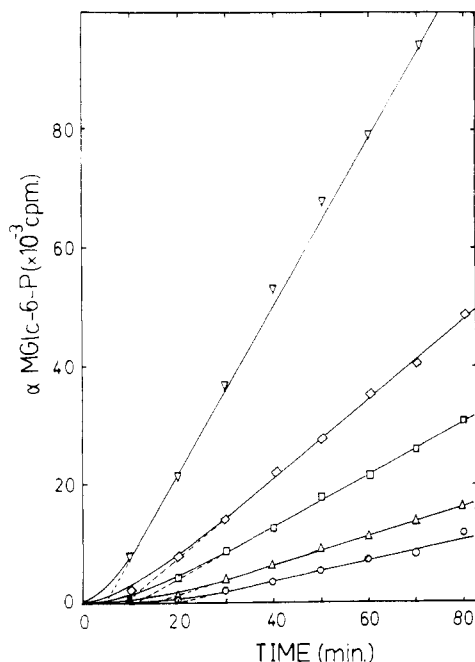


FIGURE 1: Phosphorylation of α -MeGlc as a function of time and E_1 concentration. The E_1 concentrations are ($\mu\text{g}/\text{mL}$) (\circ) 0.25, (Δ) 0.38, (\square) 0.50, (\diamond) 0.63, and (∇) 1.25. E_{II} ($20 \mu\text{L}$) was added as a membrane suspension, prepared as described under Materials and Methods.

was separated from the nonphosphorylated sugar via a column containing 1-mL bed volume Dowex Ag 1-X2 resin. The reaction mixture was loaded on the column and immediately washed with 20 mL of H_2O to remove nonphosphorylated sugar. Subsequently, the phosphorylated sugar was eluted with 12 mL of 1 M LiCl directly into scintillation vials. Emulsifier scintillator (Packard) (7.5 mL) was added and the radioactivity was counted in a Nuclear Chicago Mark I liquid scintillation counter. The counting efficiency was 60% and the background was 400–500 cpm. When the rate of phosphorylation was being measured, a single reaction vessel was used for each time curve. At stated time intervals 100 μL of the reaction mixture was pipetted directly onto a Dowex column and immediately rinsed with 20 mL of water.

Preincubation studies were executed in the following manner. Components were preincubated at 37 $^\circ\text{C}$ for 1 h in a total volume of 200 μL containing 25 mM Tris-HCl, pH 7.5, 1 mM DTT, and 1 mM NaN_3 . After preincubation, the time curve was started by adding 25 μL of buffer containing the remaining components. This procedure avoids large changes of temperature and volume in between the preincubation step and the beginning of the time curve. Such changes in volume and temperature lead to large scattering in the measured rates and lag times for reasons which will be obvious at the end of Results.

Phosphoenolpyruvate (monocyclohexylammonium salt and potassium salt) and *dithiothreitol* were purchased from Sigma Chemical Co.

Methyl α -D-[U- ^{14}C]glucopyranoside (180 $\mu\text{Ci}/\mu\text{mol}$) was purchased from the Radiochemical Centre, Amersham.

Sephacryl S-200 was purchased from Pharmacia Fine Chemicals.

Results

Lag Time Dependence on E_1 and E_{II} Concentrations. The time dependence of methyl α -glucoside phosphorylation as a function of E_1 concentration is presented in Figure 1. In these measurements E_{II} is in excess so that the rate of phosphory-

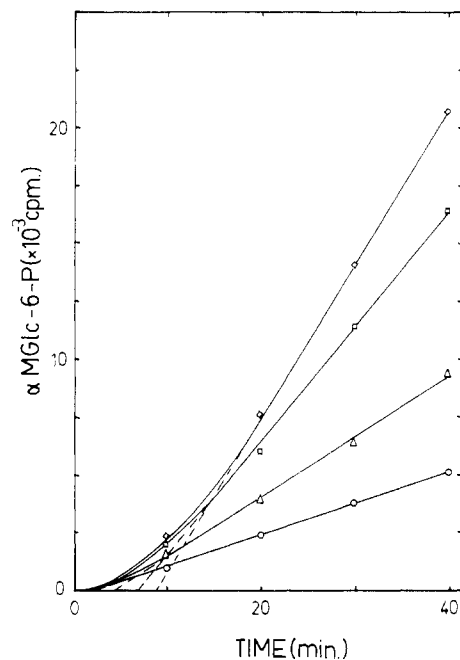


FIGURE 2: Phosphorylation of α -MeGlc as a function of time and E_{II} concentration. The E_{II} concentrations are (μL) (\circ) 0.6, (Δ) 1.2, (\square) 2.5, and (\diamond) 5.0. The E_1 concentration was 0.63 $\mu\text{g}/\text{mL}$. The time curves have been measured and were linear for 80 min. Only the first 40 min of the time curve is presented to show the effect of E_{II} on the lag time more clearly.

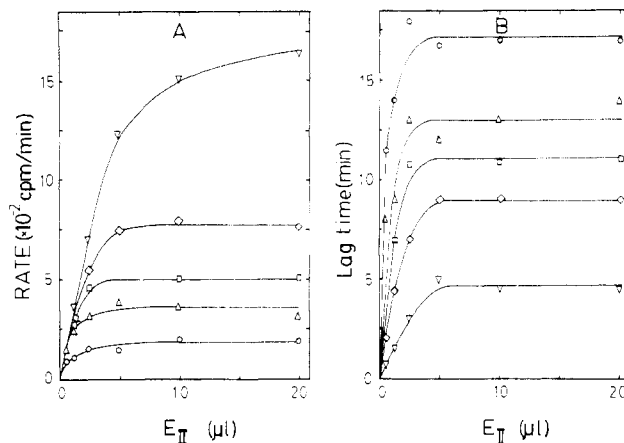


FIGURE 3: Rates of phosphorylation (A) and lag times (B) as a function of the E_{II} concentration at several E_1 concentrations ($\mu\text{g}/\text{mL}$): (\circ) 0.25, (Δ) 0.38, (\square) 0.50, (\diamond) 0.63, (∇) 1.25. The determination of the rates and the lag times from the time curves, as presented in Figures 1 and 2, is described in the text.

lation is independent of the E_{II} concentration but proportional to E_1 over a wide concentration range. All the curves in Figure 1 show an initial lag time before the steady-state rate of phosphorylation is attained. The value of the lag time is determined by extrapolating the linear portion of the time curve back to the time axis. As the E_1 concentration increases, the lag time decreases and approaches zero.

Figure 2 shows the time dependence of phosphorylation at a fixed E_1 concentration and varying concentrations of E_{II} . In this case the lag time increases with increasing E_{II} concentrations.

The rates and lag times as a function of E_{II} are summarized in Figure 3. Both the rate (Figure 3A) and the lag time (Figure 3B) increase with increasing E_{II} concentrations until they reach a maximum value which is determined by the E_1 concentration. In keeping with the data in Figure 1, these rates increase with increasing E_1 concentrations; the lag times,

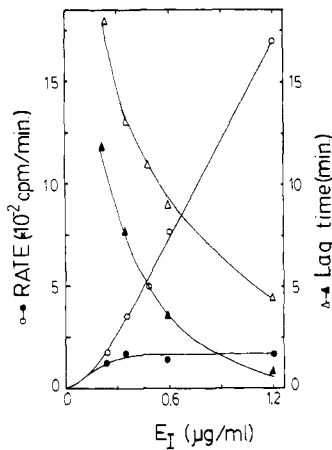


FIGURE 4: Rate of phosphorylation and the lag time as a function of the E_I concentration. E_{II} is either in excess (open symbols) or rate limiting (closed symbols). These data are replotted from Figure 3.

however, decrease. The dependence of the lag time and the rate on E_I can be more clearly seen from the data replotted in Figure 4. When the data for 0.6 and 20 μL of E_{II} from Figure 3 are plotted as a function of E_I , it is clear that there is an E_I concentration dependence in the lag time even when the rate of phosphorylation is no longer E_I concentration dependent. The relationship between the E_I and E_{II} concentrations, the rate, and the lag times will be treated under Discussion.

Preincubation Studies. In general, lag times arise from processes in which the levels of intermediates must be built up to their steady-state concentrations. These intermediates can be substrates or products in a chain of consecutive reactions or enzyme-substrate complexes or even protein-protein complexes as occur in multienzyme systems. A series of studies were executed in which various PTS proteins and substrates were preincubated in order to determine what kind of intermediates are involved in the present measurements. After preincubation the time dependence of the sugar phosphorylation activity was measured. The result presented in Figure 5 shows that the lag time decreases only if E_I is preincubated with both Mg^{2+} and PEP. Furthermore, preincubation influences only the lag time. The steady-state rate of phosphorylation remains unchanged as can be seen by comparing the linear portion of the control curve (\circ) and the curve obtained after preincubation of E_I with Mg^{2+} and PEP (∇). Preincubating E_{II} and HPr separately or together with or without E_I has no effect on the lag time. The minimum requirement to shorten the lag time is a preincubation of E_I with, at least, Mg^{2+} and PEP.

Figure 2 shows that the lag time increases with increasing E_{II} concentrations. Since this is the reverse of the concentration dependence found for E_I (Figure 1), it is necessary to consider whether the same lag time is involved for both enzymes or whether there is one process with a given lag time associated with E_I and a second process with another lag time associated with E_{II} . These two possibilities can be distinguished in the following manner. If there is only one lag time which is sensitive to the levels of both E_I and E_{II} , then a simple preincubation of E_I , Mg^{2+} , and PEP will always decrease the lag time, independent of the level of E_{II} in the subsequent assay mixture. On the other hand, if there is one lag time associated with E_I and a second associated with E_{II} , a preincubation of E_I , PEP, and Mg^{2+} alone will only eliminate that portion of the lag time associated with the E_I -related process. If the rate of phosphorylation is measured under conditions where the lag time is proportional to the E_{II} concentration, a portion of

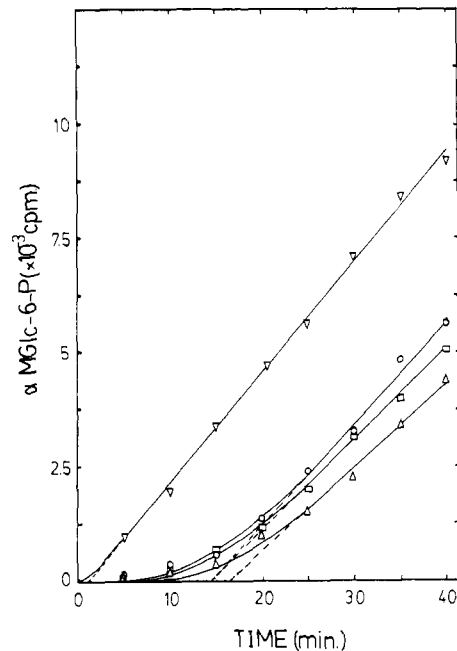


FIGURE 5: Phosphorylation of α -MeGlc as a function of time and preincubation. The following components were preincubated: (\circ) none, (Δ) E_I plus Mg^{2+} (2.5 mM), (\square) E_I plus PEP (5.0 mM), (∇) E_I plus Mg^{2+} (2.5 mM) plus PEP (5.0 mM). The preincubation was carried out as described under Materials and Methods.

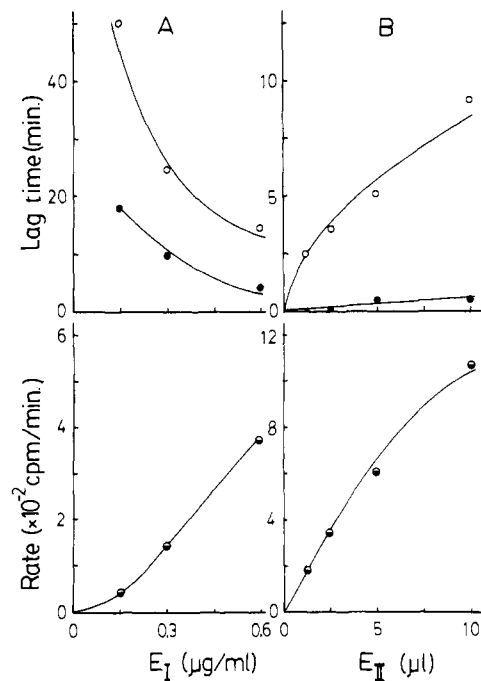


FIGURE 6: Effect of preincubation of E_I with Mg^{2+} and PEP on the lag time (upper plots) and the rate of phosphorylation (lower plots). E_I is rate limiting in (A) and E_{II} is rate limiting in (B): (\circ) not preincubated, (\bullet) preincubated.

the lag time will still be present after preincubation. In Figure 6A, the rate of phosphorylation is dependent on E_I (see lower plot). The corresponding lag time (upper plot) decreases with increasing E_I concentration. The closed circles show that the lag time can be substantially decreased or eliminated over the entire E_I concentration range by preincubating E_I with Mg^{2+} and PEP. The reciprocal experiment, measuring rates and lag times as a function of E_{II} concentration, is presented in Figure 6B. In this series both the lag time and the rate are directly proportional to the E_{II} concentration. Nevertheless, preincu-

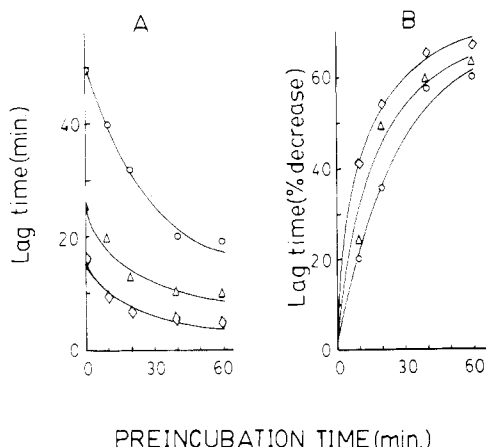


FIGURE 7: (A) Lag time as a function of the length of the preincubation of E_1 , PEP, and Mg^{2+} at rate-limiting amounts of E_1 ($\mu g/mL$): (O) 0.13, (Δ) 0.25, (\diamond) 0.50. (B) Relative decrease of the lag time obtained from the data in (A). Percent decrease = $[1 - [LT(t)/LT(t = 0)]] \times 100$, where $LT(t)$ is the lag time after preincubation time t .

bation of E_1 with PEP and Mg^{2+} eliminates the lag time. The rates of phosphorylation are the same for preincubated and nonpreincubated samples in all the measurements in Figure 6. The data presented in Figure 6 suggest that there is only one process with one lag time sensitive to the levels of both E_1 and E_{II} .

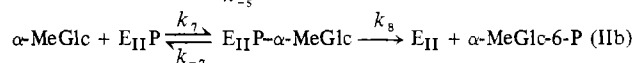
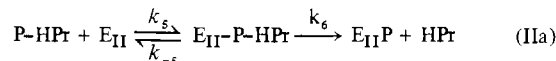
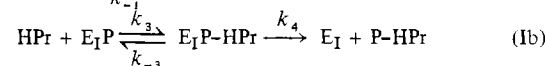
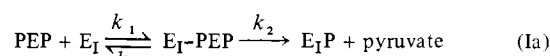
Time-Dependent Preincubation Studies. The previous sections have demonstrated an inverse relationship between the E_1 concentration and the magnitude of the lag time. In addition, preincubation studies have correlated the lag time solely with an E_1 -associated process. In this section we wish to examine the connection between the E_1 concentration and the rate of decrease of the lag time during preincubations with Mg^{2+} and PEP.

Figure 7A shows the lag time remaining after preincubation as a function of the length of preincubation time and the E_1 concentration. These data are replotted in Figure 7B to show the percent decrease in the lag time as a function of the preincubation time and E_1 concentration. It can be clearly seen, from this figure, that the rate of decrease of the lag time during preincubation is dependent on the E_1 concentration in the preincubation mixture. The higher the E_1 concentration, the more rapid the decrease in the lag time.

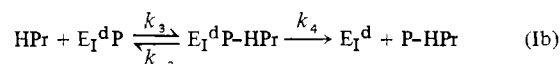
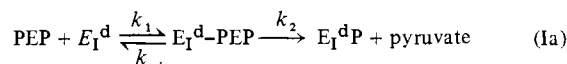
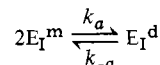
Kinetic Analysis. The observations that (1) the lag time is inversely proportional to the E_1 concentration, (2) the rate of decrease of the lag time during preincubation is proportional to the E_1 concentration, (3) the rate of phosphorylation of α -MeGlc is not entirely linear with the E_1 concentration, and (4) preincubation of only E_1 with Mg^{2+} and PEP is sufficient to decrease the lag time suggest that E_1 must be activated by PEP and Mg^{2+} and that this activation process must include an aggregation of E_1 monomers either as a result of or as a requirement for phosphorylation by Mg^{2+} and PEP. A kinetic model will be presented in the Appendix which describes these observations; it allows us to derive expressions relating the lag time to the time required to activate E_1 by a dimerization process.

As shown in Scheme I, sugar phosphorylation can be written as two enzyme-catalyzed reactions, each operating according to a bi-bi ping-pong mechanism.³ For our present consid-

Scheme I



Scheme II



erations Scheme I can be reduced to only reaction I. This can be experimentally achieved by measuring in the presence of excess E_{II} . In addition, Scheme I will be extended with a dimerization equilibrium (Scheme II).⁴

(1) **Dependence of the Total Dimer Concentration on the Concentrations of E_1 , HPr, and PEP.** The mathematical description of the reactions in Scheme II (see Appendix) is made with the assumptions that (a) only the dimer is enzymatically active (see Discussion) and (b) the association of the monomers is slow compared with reaction Ia and Ib. Therefore, the reactants in reaction I are immediately in equilibrium with the slowly increasing dimer concentration. Using the expression for the equilibrium (steady-state) value of the total dimer fraction (eq 9, Appendix)

$$\frac{2\sum[E_I^d]}{[E_I]} = 1 + \frac{1}{nA} - \frac{1}{nA}(1 + 2nA)^{1/2}$$

we see that the total dimer fraction increases with increasing n (total enzyme I concentration). More importantly, however, the total dimer fraction increases with A (increases with PEP and decreases with HPr). This relationship between the total dimer fraction and the concentrations of E_1 , PEP, and HPr will be treated under Discussion.

(2) **Dependence of the Lag Time and Steady-State Rate on the Total Dimer Concentration.** The expression for the time-dependent formation of α -MeGlc-6-P (eq 11, Appendix) has the shape of the time curves presented earlier in this section. The steady-state rate and the lag time determined from these experimental curves can also be deduced from eq 11. This equation consists of two parts. The first part is a linear function of time. The second part is an exponential function of time which decreases to zero at larger t values. The steady-state rate derived from eq 11

$$v = \frac{\frac{K_D}{8} \left[n + \frac{1}{A} - \frac{1}{A}(1 + 2nA)^{1/2} \right]}{\frac{1}{k_2} \left(1 + \frac{K_M^{\text{PEP}}}{[\text{PEP}]} \right) + \frac{1}{k_4} \left(1 + \frac{K_M^{\text{HPr}}}{[\text{HPr}]} \right)}$$

³ The reason for taking ping-pong mechanisms is the existence of phosphorylated E_1 (our unpublished results; Hengstenberg, 1977) as well as the possibility to label membranes with [³²P]PEP (Kundig, 1974) which indicates a phosphorylated E_{II} intermediate.

⁴ There is no information concerning the stoichiometry of PEP and HPr to E_1 dimer. In Scheme II we have presented the simplest case of one molecule of PEP and HPr reacting with one E_1 dimer. If the scheme proves to be different, it will not affect the qualitative behavior of the model.

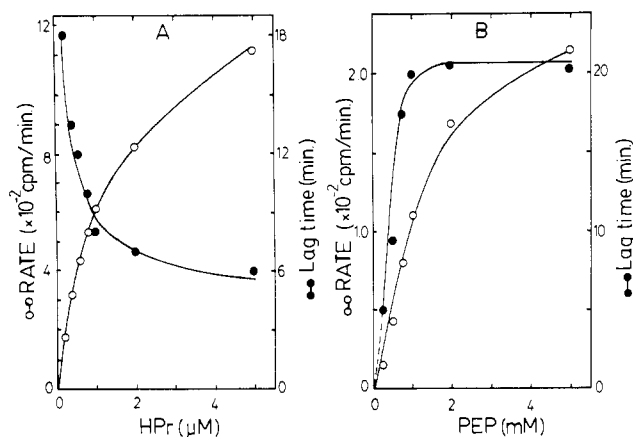


FIGURE 8: Rate of phosphorylation and the lag time as a function of HPr (A) and PEP (B). E_1 was used in a rate-limiting amount. Substrate concentrations, other than mentioned here, are given under Materials and Methods.

is similar to that for a normal bi-bi ping-pong mechanism. Only the numerator is different from a normal linear enzyme concentration term because of the dimerization equilibrium. In this case the numerator represents the total dimer concentration which is a function of the enzyme concentration and of PEP and HPr concentrations (see also eq 9 and Discussion).

The expression for the lag time as a function of enzyme, PEP, and HPr concentrations (eq 15, Appendix)

$$\text{lag time} = \frac{2}{k_a \left[n + \frac{1}{A} - \frac{1}{A} (1 + 2nA)^{1/2} \right]} \ln \left[1 + \frac{1 + nA - (1 + 2nA)^{1/2}}{2(1 + 2nA)^{1/2}} (1 - F_0) \right]$$

demonstrates that increasing the E_1 concentration (n) decreases the lag time. This is in accordance with the experimentally found effect of E_1 on the lag time (Figure 4). The calculations also show that the lag time increases with increasing A and therefore that it should increase with increasing PEP and decrease with increasing HPr concentrations. The dependence of the lag time on PEP and HPr was measured to check the predictions of this model. Figure 8 shows that, in accordance with the model, the lag time indeed increases with PEP and decreases with HPr concentrations.

Gel Filtration Studies. The kinetic model presented in the Appendix and summarized above has been derived for a dimerization of E_1 monomers. In principle, however, association to higher molecular weight oligomers could also be involved. Since preincubation of E_1 with PEP and Mg^{2+} apparently shifts the equilibrium between monomers and oligomer, gel filtration studies in the presence or absence of PEP and Mg^{2+} were performed to determine the size of the oligomer.

The elution position of E_1 on a Sephacryl column run at room temperature in the absence of PEP and Mg^{2+} is equivalent to a molecular weight of approximately 70 000.⁵ However, when E_1 is preincubated with PEP and Mg^{2+} at 37 °C for 30 min and eluted with buffer containing PEP and Mg^{2+} , it elutes as a single peak with a molecular weight of

about 134 000. Leaving out either PEP or Mg^{2+} in the preincubation and subsequent column run results in a molecular weight 70 000. This agrees well with the observation from Figure 5 that preincubation of E_1 with either PEP or Mg^{2+} cannot decrease the lag time.

When the chromatographies were carried out at 4 °C, the following results were obtained. E_1 eluted as a single peak at the monomer position when buffers lacked Mg^{2+} and PEP and no preincubation step was employed. This is identical with the results obtained at room temperature with these conditions. However, even when E_1 was first preincubated at 37 °C with Mg^{2+} and PEP and then chromatographed in the presence of PEP and Mg^{2+} at 4 °C, it still eluted as a single peak in the monomer position. This implies that the dimer which is formed at 37 °C in the presence of Mg^{2+} and PEP is cold sensitive and dissociates at 4 °C. For this reason, large changes in volume or temperature while carrying out kinetic experiments can lead to substantial scatter in the data.

Discussion

E_1 is enzymatically active in the dimeric form. This has been shown by kinetic measurements and gel chromatography. When it is purified according to our method, it is a monomer of approximately 70 000 daltons lacking enzymatic activity. The activity reappears slowly in a sugar phosphorylation assay mixture, and eventually a constant rate of phosphorylation is achieved. The activation can also be achieved simply by preincubating E_1 with PEP and Mg^{2+} . Gel filtration shows that under these circumstances the molecular weight is about 134 000. Therefore, the active form of E_1 has a molecular weight twice that of the inactive form.

Effect of E_1 and Substrate Concentrations on the Lag Time. The fraction of E_1 in the dimer form in an assay is not solely determined by the dissociation constant (K_D) and the E_1 concentration. As has been derived in the Appendix (eq 9), the total dimer fraction is also dependent on the PEP and HPr concentrations. Increasing these substrate concentrations leads to an increased total dimer concentration ($\sum [E_1^d]$) in the case of PEP and a decreased total dimer concentration in the case of HPr. The PEP and HPr dependence of the lag time as described by eq 15 and experimentally confirmed (Figure 8) can be attributed to their effect on the total dimer concentration. E_1 in the assay mixture will be located in one of three pools: monomers, free dimers, and dimer complexes (see also eq 1). Adding PEP to a given E_1 concentration will cause a disturbance in the monomer-dimer equilibrium since PEP reacts with the free dimer to form phosphorylated dimers, thus raising the dimer complex concentration. The monomer-dimer equilibrium will be restored by refilling the free dimer pool from the monomer pool. This is the slow process, resulting in the lag time in sugar phosphorylation. The addition of HPr causes dephosphorylation of the dimer complex pool and an increase in the free dimer concentration. The monomer-dimer equilibrium will now be restored by dissociation of the dimers to monomers. Therefore, the total dimer concentration decreases upon addition of HPr, and less dimer has to be formed resulting in a shorter lag time. PEP and HPr affect not only the total dimer concentration but also the rate of dimer formation. This can be seen from eq 8 which describes the monomer concentration as a function of time and the concentrations of E_1 , PEP, and HPr. Differentiation of this equation (not shown) leads to the rate of total dimer formation which increases with increasing E_1 and PEP concentrations and decreases with increasing HPr concentrations.

Increasing the E_1 concentration leads to an increment not only in the total dimer formation rate but also in the total

⁵ In contrast to our preliminary estimates of 85 000 (Robillard et al., 1979), we find a molecular weight for the E_1 monomer between 67 000 and 72 000 using either calibrated NaDodSO₄-containing polyacrylamide gels or a calibrated Sephacryl S-200 column.

dimer concentration. However, with increasing E_I concentration the lag time decreases, due to the concentration effect in the association reaction (eq 7), which is quadratic in the monomer concentration, $2k_a[E_I^m]^2$.

Influence of E_{II} on the Lag Time. Figure 3A,B shows that E_{II} only affects the lag time when it is rate determining. When its concentration is in excess, E_{II} has no effect on the lag time. When the E_{II} concentration is lower, so that it is rate limiting, E_I must be in excess; however, when E_I first enters the reaction mixture, it is in an inactive form and activates slowly by association to a dimer. Suppose two experiments are carried out with the same E_I concentration and different E_{II} concentration. In the first experiment, if we let the E_I concentration be rate limiting, the lag time will reflect the time required to form the steady-state level of the total dimers. In the second experiment, we will let E_{II} be rate limiting; now only the formation time for that amount of E_I dimers sufficient to come into excess over E_{II} will determine the lag time and that will be shorter than in the first experiment. Furthermore, the concentration of E_I dimers which are in excess over E_{II} is only determined by the E_{II} concentration. Higher rate-limiting E_{II} concentrations require higher total dimer concentrations if E_I is to be in excess. Thus, at a fixed E_I concentration, increasing E_{II} concentrations lead to increasing lag times.

The fact that, at a fixed, rate-limiting E_{II} concentration, higher E_I concentrations decrease the lag time as found in Figure 4 (closed symbols) and eq 19 can also be explained. The concentration of E_I dimers required to be in excess is only determined by the fixed, rate-limiting E_{II} concentration. The total dimer formation rate, however, increases with increasing E_I concentrations. Thus, the excess concentration of E_I will be reached faster if the total E_I concentration is higher. The result will be a decreasing lag time.

Preincubation Studies. The relative decrease of the lag time as presented in Figure 7 can be formulated by using eq 15. In a certain E_I concentration range the relative decrease of the lag time reflects the fraction of the steady-state total dimer concentration formed during preincubation (F_0). Therefore, the relative decrease of the lag time can be regarded as the total dimer formation rate. The model presented is also consistent with our observations that the steady-state rates of phosphorylation are independent of preincubation of E_I , PEP, and Mg^{2+} . Equation 14, which gives the steady-state rate as a function of enzyme and substrate concentrations, does not contain a term which represents the "start" concentration of dimers. Such a term is found, however, in the equation for the lag time (eq 15). The term F_0 represents this start concentration and, as may be expected, the lag time decreases as F_0 increases.

Conclusion

A kinetic model has been derived which explains the activation of E_I through a dimerization process which is influenced by PEP and Mg^{2+} . Physical evidence confirms this association state. The monomer/dimer ratio in the absence of PEP and Mg^{2+} has not yet been determined. Nor is there any evidence that phosphorylation rather than a simple binding of PEP and Mg^{2+} shifts the monomer-dimer equilibrium. Further study of these matters as well as a quantitative treatment of the kinetic parameters is now in progress.

Acknowledgments

We acknowledge the helpful discussions and continued interest of Dr. Dooijewaard during the execution of this work. The HPr and E_I were prepared by R. ten Hoeve-Duurkens and A. Seinen. Their technical assistance has been invaluable.

Appendix

Expression for the Dimer Concentration. By use of the mechanism presented in Scheme II (Results), the total amount of enzyme I (E_I) can be written as a summation of all forms:

$$[E_I] = [E_I^m] + 2([E_I^d] + [E_I^d\text{-PEP}] + [E_I^d\text{P}] + [E_I^d\text{P-HPr}]) \quad (1)$$

In this equation $[E_I^m]$ represents the free monomer concentration and the term in parentheses represents the total dimer concentration ($\sum[E_I^d]$) consisting of the free dimer concentration $[E_I^d]$ and the dimer complex concentrations ($[E_I^d\text{-PEP}] + [E_I^d\text{P}] + [E_I^d\text{P-HPr}]$). According to assumption b (see Scheme II, Results), the dimers are in equilibrium with each other and can be expressed in terms of the free dimer concentration $[E_I^d]$

$$[E_I^d\text{-PEP}] = \frac{[\text{PEP}]}{K_M^{\text{PEP}}} [E_I^d] \quad (2)$$

$$[E_I^d\text{P-HPr}] = \frac{k_2[\text{PEP}]}{k_4 K_M^{\text{PEP}}} [E_I^d] \quad (3)$$

$$[E_I^d\text{P}] = \frac{k_2[\text{PEP}]K_M^{\text{HPr}}}{k_4 K_M^{\text{PEP}}[\text{HPr}]} [E_I^d] \quad (4)$$

in which $K_M^{\text{PEP}} = (k_{-1} + k_2)/k_1$ and $K_M^{\text{HPr}} = (k_{-3} + k_4)/k_3$. Substitution of eq 2-4 into eq 1 gives

$$[E_I] = [E_I^m] + 2[E_I^d] \left[1 + \frac{[\text{PEP}]}{K_M^{\text{PEP}}} \left[1 + \frac{k_2}{k_4} \left(1 + \frac{K_M^{\text{HPr}}}{[\text{HPr}]} \right) \right] \right] \quad (5)$$

or

$$[E_I] = [E_I^m] + 2[E_I^d\text{P-HPr}] \left[\frac{k_4}{k_2} \left(1 + \frac{K_M^{\text{PEP}}}{[\text{PEP}]} \right) + \left(1 + \frac{K_M^{\text{HPr}}}{[\text{HPr}]} \right) \right] \quad (6)$$

The time dependence of the dimerization process is described by the differential equation

$$2 \frac{d\sum[E_I^d]}{dt} = -\frac{d[E_I^m]}{dt} = 2k_a[E_I^m]^2 - 2k_{-a}[E_I^d] \quad (7)$$

Substitution of eq 5 into eq 7, followed by integration with the boundary condition that $[E_I^m(t=0)]$ is equal to some constant, gives the expression for the monomer concentration as a function of time

$$[E_I^m] = \frac{K_D}{4A} [-1 + (1 + 2nA)^{1/2}] \left\{ [1 + n_0A + (1 + 2nA)^{1/2}] + [1 + n_0A - (1 + 2nA)^{1/2}] \exp \left[-\frac{k_{-a}}{A} (1 + 2nA)^{1/2} t \right] \right\} / \left\{ [1 + n_0A + (1 + 2nA)^{1/2}] - [1 + n_0A - (1 + 2nA)^{1/2}] \exp \left[-\frac{k_{-a}}{A} (1 + 2nA)^{1/2} t \right] \right\} \quad (8)$$

where $n_0 = 4[E_I^m(t=0)]/K_D$, $n = 4[E_I]/K_D$, $K_D = k_{-a}/k_a$, and $A = 1 + ([\text{PEP}]/K_M^{\text{PEP}})[1 + (k_2/k_4)(1 + K_M^{\text{HPr}}/[\text{HPr}])]$. The equilibrium (steady-state) value of the total dimer fraction is obtained from eq 8 by setting $t = \infty$:

$$\frac{2\sum[E_I^d]}{[E_I]} = 1 - \frac{[E_I^m(t = \infty)]}{[E_I]} = 1 + \frac{1}{nA} - \frac{1}{nA}(1 + 2nA)^{1/2} \quad (9)$$

Expression for the Reaction Velocity and the Lag Time. The initial rate of phosphorylation can be obtained from eq 6:

$$v(t) = \frac{d[\alpha\text{-MeGlc-6-P}]}{dt} = \frac{d[\text{P-HPPr}]}{dt} = k_4[E_I^d\text{P-HPPr}] = \frac{\frac{1}{2}([E_I] - [E_I^m(t)])}{\frac{1}{k_2}\left(1 + \frac{K_M^{\text{PEP}}}{[\text{PEP}]}\right) + \frac{1}{k_4}\left(1 + \frac{K_M^{\text{HPPr}}}{[\text{HPPr}]}\right)} \quad (10)$$

Substitution of eq 8 into eq 10, followed by integration with the boundary condition $[\alpha\text{-MeGlc-6-P}(t = 0)] = 0$, gives eq 11 for the concentration of $\alpha\text{-MeGlc-6-P}$ as a function of time as well as enzyme and substrate concentrations

$$[\alpha\text{-MeGlc-6-P}(t)] = \frac{1}{\frac{1}{k_2}\left(1 + \frac{K_M^{\text{PEP}}}{[\text{PEP}]}\right) + \frac{1}{k_4}\left(1 + \frac{K_M^{\text{HPPr}}}{[\text{HPPr}]}\right)} \left\{ \frac{K_D}{8} \left[n + \frac{1}{A} - \frac{1}{A}(1 + 2nA)^{1/2} \right] t - \frac{1}{4k_a} \ln \left[1 - \frac{(1 + 2nA)^{1/2} - (1 + nA)}{2(1 + 2nA)^{1/2}} (1 - F_0) \times \left[1 - \exp \left[-\frac{k_{-a}}{A}(1 + 2nA)^{1/2} \right] t \right] \right] \right\} \quad (11)$$

where $F_0 = [[E_I] - [E_I^m(t = 0)]] / [[E_I] - [E_I^m(t = \infty)]]$ which is the fraction of the equilibrium total dimer concentration already present at $t = 0$. Schematically, eq 11 can be represented by

$$[\alpha\text{-MeGlc-6-P}(t)] = at - b \ln [1 - c[1 - \exp(-dt)]] \quad (12)$$

Here a , b , c , and d are constants. As t increases, the nonlinear eq 12 approaches that of a straight line

$$[\alpha\text{-MeGlc-6-P}(t)] = at - b \ln(1 - c) \quad (13)$$

or

$$[\alpha\text{-MeGlc-6-P}(t)] = at - e$$

where e is another constant. The steady-state rate of phosphorylation is given by the coefficient a of the linear part of eq 12 and 13. The lag time is found by substituting $[\alpha\text{-MeGlc-6-P}] = 0$ into eq 13. (This is in fact the extrapolation back to the time axis as done with the experimental time curves to determine the lag time.) The lag time from eq 13 is given by

$$\text{lag time} = e/a$$

Applying this to eq 11, we get the steady-state rate

$$v = \frac{\frac{K_D}{8} \left[n + \frac{1}{A} - \frac{1}{A}(1 + 2nA)^{1/2} \right]}{\frac{1}{k_2} \left(1 + \frac{K_M^{\text{PEP}}}{[\text{PEP}]} \right) + \frac{1}{k_4} \left(1 + \frac{K_M^{\text{HPPr}}}{[\text{HPPr}]} \right)} \quad (14)$$

and the lag time

$$\text{lag time (LT)} = \frac{2}{k_{-a} \left[n + \frac{1}{A} - \frac{1}{A}(1 + 2nA)^{1/2} \right]} \ln \left[1 - \frac{(1 + 2nA)^{1/2} - (1 + nA)}{2(1 + 2nA)^{1/2}} (1 - F_0) \right] \quad (15)$$

Combined Effect of E_I and E_{II} on the Lag Time and the Rate of Phosphorylation. The observation that an E_{II} concentration dependence exists in the lag time (Figures 2 and 3) even though the lag time is solely an E_I -related process (Figures 5 and 6) can be understood if we examine the complete sequence of PTS reactions (Scheme I) and include the E_I dimerization process as the first step in this scheme. This is nothing more than lifting the earlier restriction on Scheme II that E_{II} be in excess.

Assuming that PEP and $\alpha\text{-MeGlc}$ are saturating and the rate of phosphorylation is linear with respect to p (total HPr concentration), the steady-state rate of phosphorylation is given by

$$v = \frac{p}{\frac{8K_M^{\text{HPPr}}}{K_D k_4 \left[n + \frac{1}{A} - \frac{1}{A}(1 + 2nA)^{1/2} \right]} + \frac{K_M^{\text{P-HPPr}}}{k_6[E_{II}]} \quad (16)$$

Equation 16 explains the behavior of the two enzymes determining the rate of phosphorylation as found in Figure 3A. At small E_{II} concentrations the E_{II} -containing term in the denominator is greater than the E_I (n)-containing term. This latter term can be neglected, and the rate equation reduces to

$$v = \frac{k_6}{K_M^{\text{P-HPPr}}} p [E_{II}] \quad (17)$$

At higher E_{II} , both terms contribute to the rate which then ceases to be linear with the E_{II} concentrations and begins to level off. Further increase of the E_{II} concentration makes the E_{II} -containing term in eq 16 negligible so that the maximum rate is determined by the E_I term:

$$v_{\text{max}} = \frac{k_4 K_D}{8 K_M^{\text{HPPr}}} p \left[n + \frac{1}{A} - \frac{1}{A}(1 + 2nA)^{1/2} \right] \quad (18)$$

The corresponding lag time at any combination of E_I and E_{II} concentrations is given by

$$\text{LT} = \frac{1}{k_{-a} \left[K' \frac{[E_I]^2}{[E_{II}]} + n + \frac{1}{A} - \frac{1}{A}(1 + 2nA)^{1/2} \right]} \ln \left[1 + \frac{K' \frac{[E_I]^2}{[E_{II}]} + 1 + nA - (1 + 2nA)^{1/2}}{2(1 + 2nA)^{1/2}} (1 - F_0) \right] \quad (19)$$

where $K' = k_4 K_M^{\text{P-HPPr}} / (k_6 K_M^{\text{HPPr}} K_D)$. The dependence of the lag time on E_{II} , as found in Figure 3B, is explained by eq 19. Calculations with eq 19 reveal that at rate-limiting amounts of E_{II} the lag time increases when the E_{II} concentration is raised. In this region, the lag time is also dependent upon E_I ; increasing the E_I concentration decreases the lag time. Higher E_{II} concentrations will ultimately lead to neglecting the

E_{II} -containing term in eq 19; at that point, the maximum lag time, determined solely by the E_I concentration, will be reached:

$$LT = \frac{2}{k_a \left[n + \frac{1}{A} - \frac{1}{A} (1 + 2nA)^{1/2} \right]} \ln \left[1 + \frac{1 + nA - (1 + 2nA)^{1/2}}{2(1 + 2nA)^{1/2}} (1 - F_0) \right] \quad (20)$$

It should be emphasized that in eq 19 the lag time always remains dependent on the E_I concentration even if E_{II} is very small (i.e., excess E_I). This has also been found experimentally (see Figure 4) and was explained qualitatively under Discussion.

Independent Activation of the Acetylcholine Receptor from *Torpedo californica* at Two Sites[†]

Angelo M. Delegeane and Mark G. McNamee*

ABSTRACT: Membrane vesicles enriched in acetylcholine receptor were prepared from the electroplax tissue of *Torpedo californica*. The receptor was reduced with dithiothreitol to expose a sulfhydryl group near the ligand binding site and then treated in one of the following ways: (1) affinity alkylated with bromoacetylcholine, a receptor activator, (2) affinity alkylated with maleimidobenzyltrimethylammonium, a receptor inhibitor, or (3) reoxidized to the native state with dithiobis(2-nitrobenzoate). The affinity labels blocked half of the binding sites for α -bungarotoxin. The toxin sites not protected by the affinity labels were protected by carbamylcholine based on studies of toxin binding kinetics. The functional response of native and affinity-alkylated receptors

The nicotinic acetylcholine receptor (AcChR)¹ from electroplax tissue can be affinity alkylated by 4-maleimidobenzyltrimethylammonium (MBTA) and by bromoacetylcholine (BAC), following reduction of the receptor to expose a reactive sulfhydryl group near the active site (Karlin et al., 1975; Damle et al., 1978; Moore & Raftery, 1979a). Following alkylation, MBTA acts as an irreversible inhibitor of AcChR activation in intact electroplax cells from *Electrophorus electricus* (Karlin, 1969); in contrast, BAC acts as an irreversible activator, leading to prolonged depolarization (Silman & Karlin, 1969). Both affinity labels react specifically with the 40 000 M_r subunit of AcChR from *E. electricus* and *Torpedo californica*, and this 40 000 M_r subunit (the α chain) is presumed to contain the ligand binding site(s) (Karlin et al., 1975; Damle et al., 1978). Snake α -neurotoxins, which act as nearly irreversible inhibitors of AcChR activation, also bind to the α chain [for reviews, see Heidmann & Changeux

References

- Anderson, B., et al. (1971) *J. Biol. Chem.* 246, 7023-7033.
 Dooijewaard, G., Roossien, F. F., & Robillard, G. T. (1979a) *Biochemistry* 18, 2990-2995.
 Dooijewaard, G., Roossien, F. F., & Robillard, G. T. (1979b) *Biochemistry* 18, 2996-3001.
 Hengstenberg, W. (1977) *Curr. Top. Microbiol. Immunol.* 77, 97-126.
 Kundig, W. (1974) *J. Supramol. Struct.* 2, 695-714.
 Kundig, W., & Roseman, S. (1971) *J. Biol. Chem.* 246, 1393-1406.
 Postma, P. W., & Roseman, S. (1976) *Biochim. Biophys. Acta* 457, 213-257.
 Robillard, G. T., Dooijewaard, G., & Lolkema, J. (1979) *Biochemistry* 18, 2984-2989.
 Roseman, S. (1969) *J. Gen. Physiol.* 54, 138s-180s.

was measured by a sodium ion flux procedure. In the absence of added cholinergic activators, only slow ion flux was observed. In the presence of carbamylcholine, a receptor activator, both native and modified membranes showed the increased sodium flux associated with functional receptors. The concentration of carbamylcholine required for a 50% maximal response was higher in the affinity-labeled membranes. Preincubation of the membranes with carbamylcholine blocked the increased ion flux, indicating that desensitization could be induced. The results provide evidence for the existence of two functional sites on the acetylcholine receptor. Each site corresponds to a bungarotoxin binding site and can be independently activated and desensitized.

(1978) and Barrantes (1979)]. However, there are two α -neurotoxin binding sites for each affinity-labeling site, and analysis of NaDodSO₄-polyacrylamide gel electrophoresis patterns indicates that there are at least two α subunits for each receptor monomer complex of M_r 250 000 (Karlin et al., 1975; Reynolds & Karlin, 1978). Since the binding of BAC and MBTA is mutually exclusive (Damle et al., 1978), it appears that one and only one of the two binding sites can be affinity labeled. Using a different affinity label, *p*-(trimethylammonium)benzenediazonium fluoroborate, Weiland et al. (1979) recently found a 1:1 ratio of toxin to affinity-labeled sites.

For membrane-bound AcChR, kinetic and equilibrium binding studies using toxins have not yet revealed differences between the two toxin sites (Blanchard et al., 1979). In detergent solution, however, kinetic heterogeneity has been ob-

[†] From the Department of Biochemistry and Biophysics, University of California, Davis, California 95616. Received September 27, 1979. Supported by Research Grant NS-13050 from the National Institute of Neurological and Communicative Diseases and Stroke.

¹ Abbreviations used: AcChR, acetylcholine receptor; MBTA, 4-maleimidobenzyltrimethylammonium; BAC, bromoacetylcholine; AcCh, acetylcholine; Carb, carbamylcholine; VDB, vesicle dilution buffer; DTNB, 5,5'-dithiobis(2-nitrobenzoate); DTT, dithiothreitol; PMSF, phenylmethanesulfonyl fluoride; [¹²⁵I]- α -BgTx, iodinated α -bungarotoxin.